 doi:10.20944/preprints202005.0302.v1

Type of the Paper (Article)

Oxidized and Non-Oxidized Multiwalled Carbon Nanotubes as Materials for Adsorption of Lanthanum(III) Aqueous Solutions

Francisco J. Alguacil[1], Irene García-Díaz[1], Esther Escudero Baquero[1], Olga Rodríguez Largo[1] and Félix A, López [1,*]

[1] Centro Nacional de Investigaciones Metalúrgicas (CENIM-CSIC), Avda. Gregorio del Amo 8, 28040 Madrid, Spain. fjalgua@cenim.csic.es (F.J.A.), igd@cenim.csic.es (I.G.D.), mebaquero@cenim.csic.es (E.M.B.), olga.rodriguez@csic.es (O.R.L.)

* Correspondence: f.lopez@csic.es ; Tel.: +34-91-553 89 00 (F.A.L.)

Abstract: The behaviour of oxidized and non-oxidized multiwalled carbon nanotubes in the adsorption of lanthanum(III) from aqueous solutions is described. Metal uptake is studied as a function of several variables such as the stirring speed of the system, pH of the aqueous solution and metal and nanomaterial concentrations. The experimental results are fitted to various kinetics and isotherm models, being the rate law fitted to the film diffusion and particle diffusion models, when the non-oxidized and the oxidized nanomaterials are used to remove lanthanum from the solution, respectively. Sulphuric acid solutions seem to be appropriate to recover the metal from La-loaded nanomaterials.

Keywords: lanthanum; multiwalled carbon nanotubes; adsorption; recovery

1. Introduction

Since the sixties of the last century, applications of rare earths in daily life had been increased until become to be elements which are critical in industrial developments and modern technologies, thus in this context, these elements are designed as technology-critical elements [1]. Although rare earths are more abundant than precious metals, their individual extraction is not an easy task mainly due to two main reasons; i) they are dispersed in ores, and ii) having similar chemical properties, it is difficult their individual separation.

With uses in different technologies and industries, rare earths are considered by the European Commission as the most critical raw materials group with the highest supply risk [2]. However, and in spite of their great applications and the larger amounts of REs-wastes, their recycling is still poorly developed, i.e. in the EU only 6% of the heavy REs and 7% of the light REs are recovered[3][4].

Among these elements, lanthanum is used in metal alloys, batteries, glass, catalysts, and rechargeable lithium-nickel batteries[5],[6] and it is being considered as one of the most critical elements until 2025 [7]. Particularly, the recycling of electric and hybrid vehicles batteries is of a great social and technological challenge, mainly due to the environmental problem associated to their dangerous compounds, among others, heavy metals which are forming part of the anode in the Ni-MH cell [3][8]. Nowadays, these types of batteries are one of the most used [9].

Including in separation technologies, adsorption is one of the most popular methodologies due to its simplicity, flexibility, low cost and high efficiency [10]. In the last decades, the study and the development of new adsorbent had been constant, such as clay ore, chelating, carbon nanomaterials, MOFs, hallosite nanotubes and activated carbon [11],[12],[13],[14],[15],[16],[17],[18]. Among these, carbon nanomaterials are a great research field due to their metals adsorption properties [10],[19],[20],[21],[22],[23],[24],[25],[26],[27],[28],[29]. Different researches have been conducted in the La adsorption. Crane et al. [30] studied the behavior of La adsorption onto nanoscale zero valent

 doi:10.20944/preprints202005.0302.v1

iron in an acid drainage medium; Iftekhar et al. [31] reviewed the factors that affect the La adsorption with different adsorbents, biosorbent, inorganic nano/composites, magnetic, silica, graphene oxides, activated carbon, etc... Finally, Cardoso et al. [32] also presented a deep review about the adsorption capacity of different kind carbon nanomaterials.

Since the global demand of REs is increased and it is expected to experiment a notable growth over time [33], the present investigation concerns the adsorption of lanthanum(III) from aqueous solutions with two commercial available adsorbents, in the form of, non-oxidized and oxidized (carboxylic groups) multiwalled carbon nanotubes.

2. Materials and Methods

The adsorbents used in this research (Merk KGaA, Damstadt, Germany) have the characteristics shown in Table 1.

Table 1. Characteristics of the adsorbents.

Adsorbent	Purity (%)	[a] Functionalization grade (%)	BET (m^2/g)	Average diameter (nm)	Density	Length (μm)	Method of process
MWCNT	>98%	----	263	6-9	2.1	5	CVD
ox-MWCNT	>80%	>8	307	9.5	---	1.5	CVD

[a] carboxylic groups. CVD: Chemical vapour deposition

On both adsorbents, Z potential was measured using a Zetasizer Malvern Nano ZS (Malvern, UK) at 25º C. Aqueous suspensions were prepared in pH solutions between 1 and 13 using solutions of HCl and NaOH. The concentration of activated carbon was adjusted to a value of 0.1 g/L. The suspensions were dispersed with a Bandelin Electronic Sonopuls HD 3100 sonicator (Bandelin, Berlín, Germany), using amplitudes of 60% for 150 s. The results from these measurements were shown in Figure 1, indicating that the isoelectronic points (IEP) were of 1.22 and 0.26 for the MWCNTs and ox-MWCNTs, respectively.

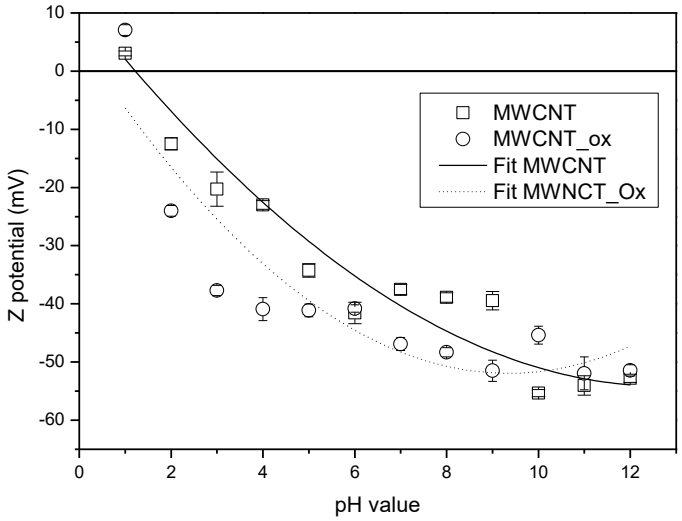

Figure 1. Z potential vs pH.

Lanthanum(III) nitrate ($La(NO_3)_3{\cdot}6H_2O$) (Merk KGaA, Damstadt, Germany) was used as source for La^{3+} ions. Other reagents were of AR grade.

Batch adsorption experiments were performed in a 0.5 L glass reactor provided of mechanical shaking, and the percentage of metal in the solution was determined by monitoring the metal concentration by Inductively coupled plasma atomic emission spectroscopy (ICP-OES) using a

Preprints (www.preprints.org) | NOT PEER-REVIEWED | Posted: 18 May 2020 doi:10.20944/preprints202005.0302.v1

Agilent 5100 (Agilent Technologies, Santa Clara, California, USA) in the aqueous solution as a function of time:

$$\% = \frac{[La]_{aq,t}}{[La]_{aq,0}} x100 \quad (1)$$

whereas the percentage of metal adsorption, onto the corresponding adsorbent, was calculated by the mass balance (Equation 1). Desorption experiments were carried out on the same basis.

3. Results

3.1. La(III) uptake by non-oxidized multiwalled carbon nanotubes (MWCNTs)

Having non-active groups, lanthanum uptake onto the present nanomaterial can be described by the next equilibrium:

$$La_{aq}^{3+} \Leftrightarrow La_{c}^{3+} \quad (2)$$

where La_{aq}^{3+} and La_{c}^{3+} represented the lanthanum ions in the aqueous solution and occupying the corresponding adsorptive sites in the carbon nanomaterial, respectively.

In all the adsorption experiments carried out with MWCNTs, a stirring speed of 500 min^{-1} was used to mix the solution and the adsorbent material. By the use of aqueous solutions containing 0.01 g L^{-1} La(III) at pH 6 and carbon dosages of 4 g/L, previous experiments showed [34]that the percentage of lanthanum uptake increased with the increase of the stirring speed from 300 min^{-1} (84% metal adsorption) until reaching a maximum (99 % metal adsorption) at the above stirring speed, indicating that a minimum value of the thickness of the aqueous phase boundary layer was reached. The increase of the stirring speed until 1000 min^{-1}, resulted in a slight decrease of the adsorption, i.e., 96% at 750 min^{-1} and 94% at 1000 min^{-1}, being this decrease attributable to the formation of local equilibria at these higher stirring speeds.

The data derived from experiments at 500 min-^{1} were used to estimate the kinetics associated to the system, and this investigation revealed that La(III) uptake onto the present MWCNT was best represented by the pseudo-second order kinetic model (r^2= 0.989) [21]:

$$\frac{t}{[La]_{c,t}} = \frac{1}{k[La]_{c,e}^{2}} + \frac{1}{[La]_{c,e}} t \quad (3)$$

where $[La]_{c,e}$ and $[La]_{c,t}$ represented the lanthanum concentrations at the equilibrium and at elapsed time, respectively, k represented the rate constant, and t being the elapsed time. From this fit, it was obtained that $[La]_{c,e}$ was of 2.8 mg/g, which fitted very well with the experimental value of 2.5 mg/g, and k of 0.16 g mg^{-1} min^{-1}. Furthermore, the fit of the data to the pseudo-second order model should be indicative of chemical activation between the adsorbent and the lanthanum ions [35],[36].

3.1.1. Influence of the aqueous pH

The influence of varying the pH of the aqueous solution on the adsorption of lanthanum by the MWCNTs was evaluated. Adsorbent dosages of 3 g/L were used. The aqueous phase contained 0.01 g/L La(III) at various pH values. Table 2 shows the results obtained from these experiments. It can be seen that the decrease of the pH value decreased the percentage of metals adsorption onto the

Preprints (www.preprints.org) | NOT PEER-REVIEWED | Posted: 18 May 2020 doi:10.20944/preprints202005.0302.v1

carbon material. This could be due to the surface charge of MWCNTs turns negative at pH value higher than the pH(IEP) 1.22, see Figure 1.

Table 2. Influence of the pH on La(III) uptake.

pH	% La(III) uptake
1	15
2	32
3	61
4	80
6	98

Temperature: 25º C. Time: 5 h

The results derived from experiments at pH 6 were used to estimate the rate law for the present system, and the results derived from these fits, indicated the La(III) uptake onto the nanomaterial was best associated to the aqueous film diffusion mechanism (r^2= 0.988) [21]:

$$\ln(1-F) = -kt \quad (4)$$

where k is the rate constant, t the elapsed time, and F the fractional approach to the equilibrium, calculated as:

$$F = \frac{[La]_{c,t}}{[La]_{c,e}} \quad (5)$$

the value of k being estimated as 0.03 min^{-1}. It should be noted here, that the aqueous film diffusion was often associated to adsorption processes obeying the pseudo-second order kinetic model [37].

3.1.2. Effect of adsorbent dosage

Figure 2 represents the results obtained for the study of the influence of the adsorbent dosage on lanthanum adsorption. The aqueous solution contained 0.01 g/L La(III) at pH 6, and the adsorbent dosages ranged from 1 to 4 g L^{-1}. The results obtained showed that the increase of the adsorbent dosage increased lanthanum adsorption, however, the effectiveness of this adsorbent for metal adsorption is constant if adsorbent dosages of 3 and 4 g L^{-1} are used.

Preprints (www.preprints.org) | NOT PEER-REVIEWED | Posted: 18 May 2020 doi:10.20944/preprints202005.0302.v1

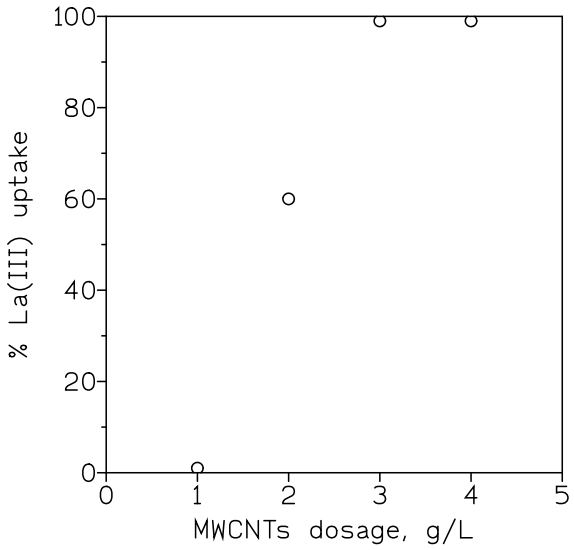

Figure 2. Influence of MWCNTs dosage on the adsorption of lanthanum. Temperature: 25º C. Time: 5h.

3.1.3. Effect of metal concentration

The influence of the initial lanthanum concentration in the percentage of adsorption of this metal onto the MWCNTs was investigated. This study was carried out using aqueous solutions that contained various lanthanum concentrations at pH 6, and carbon dosages of 3 g/L. The results are shown in Table 3, it can be seen that the percentage of metal adsorption decreased with the increase of the of the initial metal concentration in the aqueous solution, whereas maximum metal loading onto the nanomaterial was around 5.3 mg g^{-1}.

Table 3. Influence of initial metal concentration on La(III) uptake.

$[La]_0$, mg/L	% La(III) uptake	$[La]_{c,e}$, mg/g
10	98	3.3
20	75	5.0
40	46	6.1
80	20	5.3

Temperature: 25º C. Time: 5 h

These results were fitted to the Langmuir and Freundlich models [38],[39]; it was found that the best fit was related to the Langmuir Type-1 equation model (r2: 0.992), indicative of a homogeneous surface of the adsorbent covering with a single layer:

$$\frac{[La]_{aq,e}}{[La]_{c,e}} = \frac{1}{k_L [La]_{c,m}} + \frac{1}{[La]_{c,m}} [La]_{aq,e} \qquad (6)$$

Preprints (www.preprints.org) | NOT PEER-REVIEWED | Posted: 18 May 2020 doi:10.20944/preprints202005.0302.v1

in the above expression, $[La]_{c,e}$ and $[La]_{aq,e}$ represented the metal concentrations in the carbon nanomaterial and in the aqueous solution at the equilibrium, respectively, $[La]_{c,m}$ is the maximum lanthanum concentration in the carbon nanomaterial, and k_L is the Langmuir constant. From the above fit, $[La]_{c,m}$ was of 5.3 mg/g, value which compares well with the experimental value of 5.5 mg/g, and k_L being 1.4 L/mg. Moreover, being:

$$R_L = \frac{1}{1 + k_L [La]_{aq,0}} \qquad (7)$$

it was found that in all the lanthanum concentrations range used in this work, the adsorption process is favourable since $R_L<1$ [40].

3.2. La(III) uptake by oxidized multiwalled carbon nanotubes (ox-MWCNTs)

The presence of carboxylic groups in the carbon nanomaterial is indicative that La(III) uptake, onto this nanomaterial, is not represented by an adsorption process but by a cation exchange process:

$$3(R-COOH)_c + La^{3+}_{aq} \Leftrightarrow (R-COO^-)_3 La^{3+}_c + 3H^+_{aq} \qquad (8)$$

where the subscripts c and aq represented the equilibrated carbon and aqueous phases, respectively, and R the non-reactive part of the carbon nanomaterial. As it can be seen from the above equation, La(III) uptake onto the oxidized nanomaterial is accompanied by the release of protons to the aqueous solution.

3.2.1. Effect of stirring speed

A number of tests were performed in order to establish correct hydrodynamic conditions. The uptake onto the carbon material was studied as a function of the stirring speed applied to the system. Results obtained are shown in Table 4, maximum lanthanum uptake for stirring speed of 500 min^{-1} was obtained, thus, the thickness of the aqueous diffusion layer and the aqueous resistance to mass transfer were minimized. There is also a slight decrease in the metal uptake with the increase of the stirring speed, being this effect explained as above; however, in the present case, the stirring speed has an influence on the time to reach equilibrium, since, in the present experimental conditions, it is attained at 30 min (500 min^{-1}), 3 h (750 min^{-1}) and 5 h (1000 min^{-1}).

The estimation of the kinetic model, responsible for La(III) uptake onto the carbonaceous nanomaterial, indicated that the results at 500 min^{-1} best fitted to the pseudo-second order kinetic model (r^2= 0.995) [21] eq.(3), and from this, $[La]_{c,e}$ is of 10.9 mg/g, concentration which is a little higher than the maximum theoretical of 10 mg/g, which can be derived using the present experimental conditions, and higher than the more realistic and experimentally obtained of 9.9 mg/g. From this fit, and using this 9.9 mg/g value, k resulted as 0.68 g/mg min.

Preprints (www.preprints.org) | NOT PEER-REVIEWED | Posted: 18 May 2020 doi:10.20944/preprints202005.0302.v1

Table 4. Influence of the stirring speed on lanthanum uptake onto ox-MWCNTs.

Stirring speed (min^{-1})	% La(III) uptake
250	70
350	90
500	99
750	97
1000	94

Aqueous phase: 0.01 g/L La(III) at pH 6. Carbon dosage: 1 g/L. Temperature: 25º C. Time : 5h

3.2.2. Effect of the aqueous pH

Experiments were carried out using solutions of 0.01 g/L La(III) at various pH values and carbon dosages of 0.5 g/L. Figure 3 shows the results obtained; as expected from eq. (6), it can be seen that the variation of the aqueous pH value has a markedly effect on La(III) uptake onto the ox-MWCNTs, decreasing the metal uptake as the pH value is being decreasing. From eq. (6):

$$K = \frac{\left[\left(R-COO^{-}\right)_3 La^{3+}\right]\left[H^{+}\right]^3}{\left[\left(R-COOH\right)\right]^3\left[La^{3+}\right]} \qquad (9)$$

By definition, the metal distribution coefficient is:

$$D = \frac{\left[\left(R-COO^{-}\right)_3 La^{3+}\right]}{\left[La^{3+}\right]} \qquad (10)$$

substituting the above in eq.(9) and rearranging, the next expression is derived:

$$\log D = \log\left[R-COOH\right]^3 + 3pH \qquad (11)$$

thus, by plotting log D versus pH a straight line of slope 3 may be obtained. From results showed in Fig.3, such a plot confirming a slope of near 3, and that La(III) uptake onto these ox-MWCNTs occurred via the equilibrium showed in eq. (6). It is worth to note here, that the curve has an approximate S-shape, characteristic among others, of cationic exchangers.

The results at pH 6 are used to estimate the rate law for the lanthanum uptake onto these oxidized nanomaterials. The results fitted well with the particle diffusion model (r^2= 0.945) [21]:

$$\ln\left(1-F^2\right) = -kt \qquad (12)$$

and k estimated as 0.06 min^{-1}.

Preprints (www.preprints.org) | NOT PEER-REVIEWED | Posted: 18 May 2020 doi:10.20944/preprints202005.0302.v1

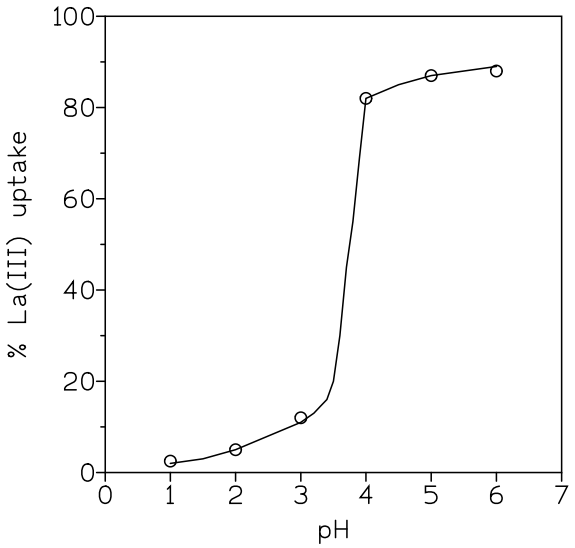

Figure 3. Variation in the percentage of La(III) adsorption versus pH. Temperature: 25º C. Time: 5 h.

3.2.3. Effect of ox-MWCNTs dosage

The variation in the percentage of lanthanum adsorption at different adsorbent dosages is shown in Fig, 4. The experiments were carried out with carbon dosages in the 0.13 to 1 g/L range and aqueous solutions of 0.01 g/L La(III) at pH 6.

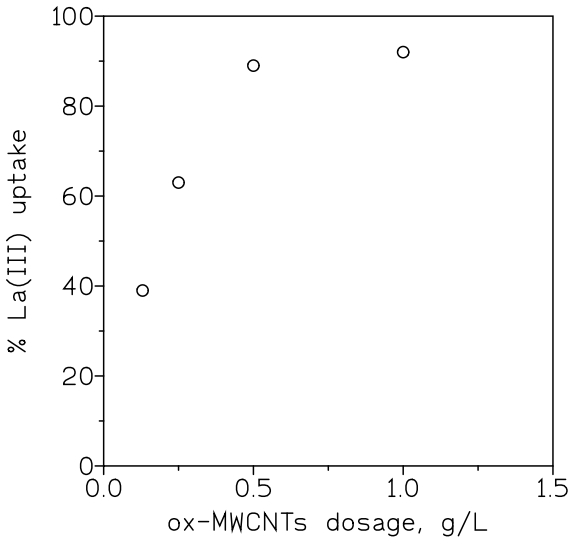

Figure 4. Influence of ox-MWCNTs dosage on the adsorption of lanthanum. Temperature: 25º C. Time: 5h.

The results obtained showed that increasing the adsorbent dosage increased the percentage of lanthanum adsorption although from 0.5 g/L carbon dosage, the difference in the values is less significant than in the lower adsorbent dosage range.

3.2.4. Effect of initial lanthanum concentration

Figure 5 shows the variation in the percentage of lanthanum uptake onto the ox-MWCNTs against the initial concentration of the metal ranging from 0.01 to 0.08 g/L. It can be observed that with the

Preprints (www.preprints.org) | NOT PEER-REVIEWED | Posted: 18 May 2020 doi:10.20944/preprints202005.0302.v1

present experimental conditions, the percentage of metal uptake reached a maximum at 0.01-0.02 g/L La(III), and then decreased.

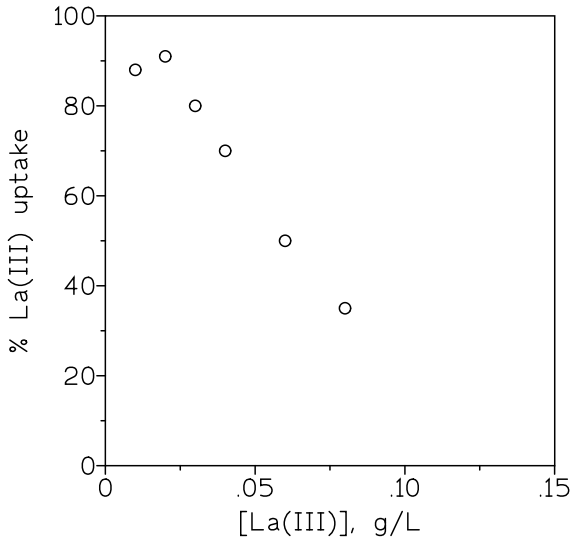

Figure 5. Influence of the initial metal concentration on the uptake of lanthanum. Aqueous phase: La(III) at pH 6. Adsorbent dosage: 0.5 g/L. Temperature: 25º C. Time. 5 h.

Lanthanum uptake is best represented by the Langmuir Type-1 isotherm (eq. (6)), with $[La]_{c,m}$ of 59 mg/g, value very similar to that experimentally obtained of 57 mg/g, and k_L 0.78 L/mg. Considering eq. (7), the estimated value of R_L for the system is of 0.11, indicative of a favourable metal uptake process [40].

3.3.Elution

As results in subsections 3.1.1. and 3.2.2. shown, using both adsorbent, there is a strong influence of the aqueous pH on lanthanum adsorption, thus, it is logical to use acidic solutions to desorbed this metal form La-loaded carbon nanomaterials. These series of experiments are carried out, at 25º C, using 0.1 M H_2SO_4 solutions, and a La-loaded nanomaterial in a 0.4 carbon/solution relationship. The results from these experiments show that the percentage of lanthanum recovery in the eluate is 79% and 87% for the non-oxidized and the oxidized nanomaterials, respectively. At the same time, the nanomaterial is recovered for further use, in the case of the oxidized nanomaterial by shifting of the equilibrium shows in eq,(6) to the left, as a consequence of the desorption reaction. The use of HCl or HNO_3 solutions do not improve the desorption results yielded with the sulphuric acid one.

4. Conclusions

From the experimental data obtained from this investigation, it can be deduced that both oxidized and non-oxidized multiwalled carbon nanotubes, commercially available materials, can be used to recover lanthanum from aqueous solutions.

For both nanomaterials, the adsorption of lanthanum, is influence by a number of variables, such as metal concentration and adsorbent dosages, the stirring speed applied to the system, and the pH of the aqueous solution.

In both cases, the metal uptake responded to the pseudo-second order kinetic model and the Langmuir Type-1 isotherm model, however, they differ in the rate law, as the film diffusion model fitted the uptake when the non-oxidized material is used, against the fitting of the particle diffusion model to the results yielded when the oxidized carbon nanotubes are used to remove lanthanum from the solution. The mechanism from which lanthanum is removed from the solution using both nanomaterials also appeared to be different: an adsorption process in the case of the non-oxidized

carbon against a cation exchange process in the case of the oxidized material. This is somewhat reflected in the fact that to obtain the same degree of lanthanum removal from the solution (more than 90%), the material dosage using the oxidized material is three times lower than that of the non-oxidized carbon nanotubes. Lanthanum loaded, onto both nanomaterials, can be desorbed by the use of acid solutions, i.e. sulphuric acid.

Author Contributions: Conceptualization, F.J.A. and F.A.L.; methodology, F.J.A. and F.A.L.; formal analysis, I.G.D and F.J.A.; investigation, F.J.A.,F.A.L., I.G.D., E.E.B. and O.R.L.; resources, F.A.L.; writing—original draft preparation, F.J.A.; writing—review and editing, F.J.A.;F.A.L.;I.G.D.E.E.B. and O.R.L. All authors have read and agreed to the published version of the manuscript

Funding: This research has received funding from the European Union's Horizon 2020 research and innovation program under grant agreement No 776851 (CarEService).

Acknowledgments: We acknowledge support of the publication fee by the CSIC Open Access Publication Support Initiative through its Unit of Information Resources for Research (URICI). The authors thank Mrs. E. Moroño for her assistance in analytical determinations through ICP-OES.

Conflicts of Interest: The authors declare no conflict of interest

References

1. Klinger, J. M. A historical geography of rare earth elements: From discovery to the atomic age. *Extr. Ind. Soc.* **2015**, *2*, 572–580, doi:10.1016/j.exis.2015.05.006.

2. EU Report on critical raw materials and the circular economy - Publications Office of the EU.

3. Omodara, L.; Pitkäaho, S.; Turpeinen, E.-M.; Saavalainen, P.; Oravisjärvi, K.; Keiski, R. L. Recycling and substitution of light rare earth elements, cerium, lanthanum, neodymium, and praseodymium from end-of-life applications - A review. *J. Clean. Prod.* **2019**, *236*, 117573, doi:10.1016/j.jclepro.2019.07.048.

4. Jowitt, S. M.; Werner, T. T.; Weng, Z.; Mudd, G. M. Recycling of the rare earth elements. *Curr. Opin. Green Sustain. Chem.* **2018**, *13*, 1–7, doi:10.1016/j.cogsc.2018.02.008.

5. Kołodyńska, D.; Hubicki, Z.; Fila, D. Recovery of rare earth elements from acidic solutions using macroporous ion exchangers. *Sep. Sci. Technol.* **2019**, *54*, 2059–2076, doi:10.1080/01496395.2019.1604753.

6. Binnemans, K.; Jones, P. T.; Blanpain, B.; Van Gerven, T.; Yang, Y.; Walton, A.; Buchert, M. Recycling of rare earths: a critical review. *J. Clean. Prod.* **2013**, *51*, 1–22, doi:10.1016/j.jclepro.2012.12.037.

7. Jacinto, J.; Henriques, B.; Duarte, A. C.; Vale, C.; Pereira, E. Removal and recovery of Critical Rare Elements from contaminated waters by living Gracilaria gracilis. *J. Hazard. Mater.* **2018**, *344*, 531–538, doi:10.1016/j.jhazmat.2017.10.054.

8. Korkmaz, K.; Alemrajabi, M.; Rasmuson, Å. C.; Forsberg, K. M. Separation of valuable elements from NiMH battery leach liquor via antisolvent precipitation. *Sep. Purif. Technol.* **2020**, *234*, 115812, doi:10.1016/j.seppur.2019.115812.

9. Fila, D.; Hubicki, Z.; Kołodyńska, D. Recovery of metals from waste nickel-metal hydride

batteries using multifunctional Diphonix resin. *Adsorption* **2019**, *25*, 367–382, doi:10.1007/s10450-019-00013-9.

10. García-Díaz, I.; López, F.; Alguacil, F. Carbon Nanofibers: A New Adsorbent for Copper Removal from Wastewater. *Metals (Basel).* **2018**, *8*, 914, doi:10.3390/met8110914.

11. Zhang, H.; Tangparitkul, S.; Hendry, B.; Harper, J.; Kim, Y. K.; Hunter, T. N.; Lee, J. W.; Harbottle, D. Selective separation of cesium contaminated clays from pristine clays by flotation. *Chem. Eng. J.* **2019**, *355*, 797–804, doi:10.1016/j.cej.2018.07.135.

12. Danyliuk, N.; Tomaszewska, J.; Tatarchuk, T. Halloysite nanotubes and halloysite-based composites for environmental and biomedical applications. *J. Mol. Liq.* **2020**, *309*, 113077, doi:10.1016/j.molliq.2020.113077.

13. Haldar, D.; Duarah, P.; Purkait, M. K. MOFs for the treatment of arsenic, fluoride and iron contaminated drinking water: A review. *Chemosphere* **2020**, *251*, 126388, doi:10.1016/j.chemosphere.2020.126388.

14. Nuithitikul, K.; Phromrak, R.; Saengngoen, W. Utilization of chemically treated cashew-nut shell as potential adsorbent for removal of Pb(II) ions from aqueous solution. *Sci. Rep.* **2020**, *10*, 3343, doi:10.1038/s41598-020-60161-9.

15. Dutta, S.; Manna, K.; Srivastava, S. K.; Gupta, A. K.; Yadav, M. K. Hollow Polyaniline Microsphere/Fe3O4 Nanocomposite as an Effective Adsorbent for Removal of Arsenic from Water. *Sci. Rep.* **2020**, *10*, 4982, doi:10.1038/s41598-020-61763-z.

16. Lapo, B.; Bou, J. J.; Hoyo, J.; Carrillo, M.; Peña, K.; Tzanov, T.; Sastre, A. M. A potential lignocellulosic biomass based on banana waste for critical rare earths recovery from aqueous solutions. *Environ. Pollut.* **2020**, *264*, 114409, doi:10.1016/j.envpol.2020.114409.

17. Renu; Agarwal, M.; Singh, K. Heavy metal removal from wastewater using various adsorbents: a review. *J. Water Reuse Desalin.* **2017**, *7*, 387–419, doi:10.2166/wrd.2016.104.

18. Alcaraz, L.; Escudero, M. E.; Alguacil, F. J.; Llorente, I.; Urbieta, A.; Fernández, P.; López, F. A. Dysprosium Removal from Water Using Active Carbons Obtained from Spent Coffee Ground. *Nanomaterials* **2019**, *9*, 1372, doi:10.3390/nano9101372.

19. Sadeghi, M. H.; Tofighy, M. A.; Mohammadi, T. One-dimensional graphene for efficient aqueous heavy metal adsorption: Rapid removal of arsenic and mercury ions by graphene oxide nanoribbons (GONRs). *Chemosphere* **2020**, *253*, 126647, doi:10.1016/j.chemosphere.2020.126647.

20. Lu, F.; Astruc, D. Nanomaterials for removal of toxic elements from water. *Coord. Chem. Rev.* **2018**, *356*, 147–164, doi:10.1016/j.ccr.2017.11.003.

21. Alguacil, F. J.; Lopez, F. A.; Rodriguez, O.; Martinez-Ramirez, S.; Garcia-Diaz, I. Sorption of indium (III) onto carbon nanotubes. *Ecotoxicol. Environ. Saf.* **2016**, *130*, 81–86,

doi:10.1016/j.ecoenv.2016.04.008.

22. Alguacil, F. J.; Garcia-Diaz, I.; Lopez, F.; Rodriguez, O. Removal of Cr(VI) and Au(III) from aqueous streams by the use of carbon nanoadsorption technology. *Desalin. WATER Treat.* **2017**, *63*, 351–356, doi:10.5004/dwt.2017.0264.

23. Liu, H.; Qiu, H. Recent advances of 3D graphene-based adsorbents for sample preparation of water pollutants: A review. *Chem. Eng. J.* **2020**, *393*, 124691, doi:10.1016/j.cej.2020.124691.

24. Vilardi, G.; Mpouras, T.; Dermatas, D.; Verdone, N.; Polydera, A.; Di Palma, L. Nanomaterials application for heavy metals recovery from polluted water: The combination of nano zero-valent iron and carbon nanotubes. Competitive adsorption non-linear modeling. *Chemosphere* **2018**, *201*, 716–729, doi:10.1016/j.chemosphere.2018.03.032.

25. Alguacil, F. J.; López, F. A. On the Active Adsorption of Chromium(III) from Alkaline Solutions Using Multiwalled Carbon Nanotubes. *Appl. Sci.* **2019**, *10*, 36, doi:10.3390/app10010036.

26. J. Alguacil, F.; A. Lopez, F. Removal of Cr(VI) from Waters by Multi-Walled Carbon Nanotubes: Optimization and Kinetic Investigations. In *Water and Wastewater Treatment*; IntechOpen, 2019.

27. Alguacil, F. Adsorption of Gold(I) and Gold(III) Using Multiwalled Carbon Nanotubes. *Appl. Sci.* **2018**, *8*, 2264, doi:10.3390/app8112264.

28. Alguacil, F. J.; Lopez, F. A.; Garcia-Diaz, I. Extracting metals from aqueous solutions using Ti-based nanostructures: a review. *Desalin. Water Treat.* **2016**, *57*, 17603–17615, doi:10.1080/19443994.2015.1087885.

29. Alguacil, F. J.; Cerpa, A.; Lado, M. I.; López, F. Extracting Metals with Carbon Nanotubes: Environmental Possibilities. *Key Eng. Mater.* **2015**, *663*, 157–165, doi:10.4028/www.scientific.net/KEM.663.157.

30. Crane, R. A.; Sapsford, D. J. Sorption and fractionation of rare earth element ions onto nanoscale zerovalent iron particles. *Chem. Eng. J.* **2018**, *345*, 126–137, doi:10.1016/j.cej.2018.03.148.

31. Iftekhar, S.; Ramasamy, D. L.; Srivastava, V.; Asif, M. B.; Sillanpää, M. Understanding the factors affecting the adsorption of Lanthanum using different adsorbents: A critical review. *Chemosphere* **2018**, *204*, 413–430, doi:10.1016/j.chemosphere.2018.04.053.

32. Cardoso, C. E. D.; Almeida, J. C.; Lopes, C. B.; Trindade, T.; Vale, C.; Pereira, E. Recovery of Rare Earth Elements by Carbon-Based Nanomaterials—A Review. *Nanomaterials* **2019**, *9*, 814, doi:10.3390/nano9060814.

33. Goodenough, K. M.; Wall, F.; Merriman, D. The Rare Earth Elements: Demand, Global Resources, and Challenges for Resourcing Future Generations. *Nat. Resour. Res.* **2018**, *27*, 201–

216, doi:10.1007/s11053-017-9336-5.

34. García Díaz, I.; Alguacil, F.J.; Escudero, E.; López, F. A. Evaluation of La (III) and Ce(III) Adsorption from Aqueous Solution Using Carbon Nanotubes Adsorbent. *Preprints2020* **2020**, *2020010254*, doi:10.20944/preprints202001.0254.v1.

35. BIOSORPTION, ISOTHERM AND KINETIC PROPERTIES OF COMMON TEXTILE DYE BY PHORMIDIUM ANIMALE. *Glob. NEST J.* **2019**, doi:10.30955/gnj.002984.

36. Amin, M. T.; Alazba, A. A.; Manzoor, U. A Review of Removal of Pollutants from Water/Wastewater Using Different Types of Nanomaterials. *Adv. Mater. Sci. Eng.* **2014**, *2014*, 1–24, doi:10.1155/2014/825910.

37. Hubbe, M. A.; Azizian, S.; Douven, S. Implications of Apparent Pseudo-Second-Order Adsorption Kinetics onto Cellulosic Materials: A Review. *Bioresour. Vol 14, No 3* **2019**.

38. Langmuir, I. THE ADSORPTION OF GASES ON PLANE SURFACES OF GLASS, MICA AND PLATINUM. *J. Am. Chem. Soc.* **1918**, *40*, 1361–1403, doi:10.1021/ja02242a004.

39. Freundlich, H. Über die Adsorption in Lösungen. *Zeitschrift für Phys. Chemie* **1907**, *57U*, doi:10.1515/zpch-1907-5723.

40. Foo, K. Y.; Hameed, B. H. Insights into the modeling of adsorption isotherm systems. *Chem. Eng. J.* **2010**, *156*, 2–10, doi:10.1016/j.cej.2009.09.013.